Electronic Transactions on Numerical Analysis.
Volume 32, pp. 17-32, 2008.

ISSN 1068-9613.

ETNA
Kent State University
etna@mcs.kent.edu

ON A MIXED DISCONTINUOUS GALERKIN METHOD*

MIKA JUNTUNEN† AND ROLF STENBERG†

Abstract. For the model Poisson problem we study the stabilized Bassi-Rebay discontinuous Galerkin method. The method is written in a mixed formulation, in which independent and fully discontinuous basis functions are used both for the scalar unknown and its flux. The continuity requirement is imposed by Nitsche's technique [Abh. Math. Sem. Univ. Hamburg, 36 (1970/71), pp. 9–15]. In the implementation the flux is then eliminated by local condensing. We show that the method is stable and optimally convergent for all positive values of the stability parameter. We also perform an a posteriori error analysis. The theoretical results are verified by numerical computations.

Key words. mixed method, discontinuous Galerkin method, stability, Nitsche's method

AMS subject classifications. 65N30, 65N55

1. Introduction.

The purpose of this paper is to study the so-called stabilized Bassi-Rebay (SBR) discontinuous Galerkin (DG) finite element method [2, 3]. In [3] a general framework for DG methods is developed and it is shown that the stability and a priori error analysis of the SBR method is covered by this.

In this contribution we will give an (alternative) a priori and an a posteriori error analysis of the method. In addition, we report on benchmark computations. First, we recall the SBR method. It is written as a mixed formulation in which the flux variable is taken as an independent unknown, fully discontinuous between elements. This flux is an auxiliary unknown that is condensed at each element at a negligible cost. Next, we give a straightforward a priori analysis, which directly shows that the method is stable for all positive values of the stability parameter. We recall that for the standard DG the lower bound is given by a constant in a discrete trace inequality, cf. [7, 8]. (In this respect, the situation is completely analogous with Galerkin-Least-Squares methods for the Stokes problem [5], where a similar phenomenon occurs.) Then, we show that the techniques for the a posteriori analysis of nonconforming methods [1, 4] can be used for the SBR method as well. Finally, we show the results of computations with the method.

2. The model problem and the discontinuous Galerkin method.

Our model problem is the mixed form of the Poisson equation, for which we present the SBR discontinuous Galerkin method. The continuity in the variational formulation is imposed weakly using the Nitsche method. For simplicity we restrict ourselves to two dimensions.

Let $\Omega \subset \mathbb{R}^2$ be a bounded domain with a piecewise smooth boundary $\partial\Omega$. With $\mathcal{T}_h$ we denote the mesh, i.e. the partitioning of Ω into triangles. With $\mathcal{E}_{\partial\Omega}$ we denote the edges of the triangles that lie on the boundary $\partial\Omega$ and with $\mathcal{E}_{\text{int}}$ we denote the internal edges of the mesh. We assume that the boundary $\partial\Omega$ is split into two non-overlapping parts Γ_D and Γ_N. The edges on the boundary are grouped into those on the Dirichlet and Neumann part, i.e., $\mathcal{E}_{\partial\Omega} = \mathcal{E}_D \cup \mathcal{E}_N$. In addition, we denote with h_T the diameter of the element $T \in \mathcal{T}_h$ and with h_E the diameter of $E \in \mathcal{E}_{\text{int}} \cup \mathcal{E}_{\partial\Omega}$. For the mesh we assume that there exists $C_1, C_2 > 0$, such that

$$C_1 h_E \leq h_T \leq C_2 h_E \quad \forall E \subset \partial T,\, \forall T \in \mathcal{T}_h.$$

*Received November 28, 2007. Accepted for publication June 9, 2008. Published online on October 21, 2008. Recommended by B. Heinrich.

†Helsinki University of Technology, Institute of Mathematics, P.O. Box 1100, FI-02015 TKK, Finland (mika.juntunen@tkk.fi).

ETNA
Kent State University
etna@mcs.kent.edu

We solve the problem

$$
\begin{aligned}
-\Delta u &= f && \text{in } \Omega,\\
u &= u_0 && \text{on } \Gamma_D,\\
\nabla u \cdot \boldsymbol{n} &= g && \text{on } \Gamma_N,
\end{aligned}
\tag{2.1}
$$

in which the load $f \in L^2(\Omega)$, $u_0 \in H^{1/2}(\Gamma_D)$ and $g \in L^2(\Gamma_N)$. Instead of solving (2.1) directly, we pose the problem in an equivalent mixed form

$$
\begin{aligned}
\boldsymbol{\sigma} - \nabla u &= 0 && \text{in } \Omega,\\
\nabla \cdot \boldsymbol{\sigma} + f &= 0 && \text{in } \Omega,\\
u &= u_0 && \text{on } \Gamma_D,\\
\boldsymbol{\sigma} \cdot \boldsymbol{n} &= g && \text{on } \Gamma_N.
\end{aligned}
\tag{2.2}
$$

Next we derive a discrete form for (2.2). We begin with the definition of the finite element spaces:

$$
\begin{aligned}
V_h &:= \{ v \in L^2(\Omega) \mid v_{|T} \in \mathcal{P}_k(T)\ \forall T \in \mathcal{T}_h \},\\
W_h &:= \{ \boldsymbol{v} \in [L^2(\Omega)]^2 \mid \boldsymbol{v}_{|T} \in [\mathcal{P}_{k-1}(T)]^2\ \forall T \in \mathcal{T}_h \},
\end{aligned}
$$

in which $\mathcal{P}_k(T)$ denotes the polynomials of order k on T. Multiplying the first equation in (2.2) with a test function $\boldsymbol{\tau} \in W_h$ and integrating over the domain Ω yields

$$
\big(\boldsymbol{\sigma}, \boldsymbol{\tau}\big)_\Omega - \big(\nabla u, \boldsymbol{\tau}\big)_\Omega = 0. \tag{2.3}
$$

Multiplying the second equation of (2.2) with a test function $v \in V_h$ and integrating by parts we get

$$
\begin{aligned}
\big(-f, v\big)_\Omega &= \sum_{T \in \mathcal{T}_h} \big(\nabla \cdot \boldsymbol{\sigma}, v\big)_T = \sum_{T \in \mathcal{T}_h} \big\{ -\big(\boldsymbol{\sigma}, \nabla v\big)_T + \big\langle \boldsymbol{\sigma} \cdot \boldsymbol{n}, v \big\rangle_{\partial T} \big\}\\
&= \sum_{T \in \mathcal{T}_h} -\big(\boldsymbol{\sigma}, \nabla v\big)_T + \sum_{E \in \mathcal{E}_{\text{int}}} \big\langle \{\boldsymbol{\sigma} \cdot \boldsymbol{n}\}, [\![v]\!] \big\rangle_E\\
&\quad + \sum_{E \in \mathcal{E}_D} \big\langle \boldsymbol{\sigma} \cdot \boldsymbol{n}, v \big\rangle_E + \sum_{E \in \mathcal{E}_N} \big\langle g, v \big\rangle_E,
\end{aligned}
\tag{2.4}
$$

in which we have employed the continuity of the normal component of the flux and used the notation

$$
\begin{aligned}
\{\boldsymbol{\sigma} \cdot \boldsymbol{n}\} &:= \frac{1}{2}(\boldsymbol{\sigma}_1 + \boldsymbol{\sigma}_2) \cdot \boldsymbol{n}_1,\\
[\![v]\!] &:= v_1 - v_2.
\end{aligned}
$$

Above, the subindices denote the functions on triangles T_1 and T_2 sharing an edge E and $\boldsymbol{n}_1$ denotes the outward pointing normal vector of T_1.

Neither the Dirichlet boundary condition nor the continuity are imposed in the solution spaces. Therefore, we need to enforce them in the variational form. Since the correct solution u is continuous and fulfils $u_{|\Gamma_D} = u_0$, it holds

$$
\sum_{E \in \mathcal{E}_{\text{int}}} -\frac{\gamma}{h_E} \big\langle [\![u]\!], [\![v]\!] \big\rangle_E = 0 \quad \text{and} \tag{2.5}
$$

$$
\sum_{E \in \mathcal{E}_D} -\frac{\gamma}{h_E} \big\langle u, v \big\rangle_E = \sum_{E \in \mathcal{E}_D} -\frac{\gamma}{h_E} \big\langle u_0, v \big\rangle_E, \tag{2.6}
$$

ETNA
Kent State University
etna@mcs.kent.edu

in which we have introduced the positive stability parameter $\gamma > 0$. (2.5) enforces the continuity and (2.6) enforces the Dirichlet boundary condition. The model problem is symmetric, and thus it is logical to maintain this also in the variational form. Once again due to the continuity and the Dirichlet boundary conditions we have

$$\sum_{E\in\mathcal{E}_{\text{int}}} \big\langle\{\boldsymbol{\tau}\cdot\boldsymbol{n}\}, [\![u]\!]\big\rangle_E = 0 \quad \text{and} \tag{2.7}$$

$$\sum_{E\in\mathcal{E}_D} \big\langle\boldsymbol{\tau}\cdot\boldsymbol{n}, u\big\rangle_E = \sum_{E\in\mathcal{E}_D} \big\langle\boldsymbol{\tau}\cdot\boldsymbol{n}, u_0\big\rangle_E. \tag{2.8}$$

Combining (2.3)–(2.8) yields the stabilized Bassi-Rebay method [3].
The SBR Method. *Find $(u_h, \boldsymbol{\sigma}_h) \in V_h \times W_h$, such that*

$$a(u_h, \boldsymbol{\sigma}_h; v, \boldsymbol{\tau}) = \mathcal{L}(v, \boldsymbol{\tau}) \quad \forall (v, \boldsymbol{\tau}) \in V_h \times W_h, \tag{2.9}$$

in which

$$\begin{aligned} a(u, \boldsymbol{\sigma}; v, \boldsymbol{\tau}) := & \sum_{T\in\mathcal{T}_h} \big[(\boldsymbol{\sigma}, \boldsymbol{\tau})_T - (\nabla u, \boldsymbol{\tau})_T - (\boldsymbol{\sigma}, \nabla v)_T\big] \\ & + \sum_{E\in\mathcal{E}_{int}} \big[\big\langle\{\boldsymbol{\sigma}\cdot\boldsymbol{n}\}, [\![v]\!]\big\rangle_E + \big\langle\{\boldsymbol{\tau}\cdot\boldsymbol{n}\}, [\![u]\!]\big\rangle_E\big] \\ & + \sum_{E\in\mathcal{E}_D} \big[\big\langle\boldsymbol{\sigma}\cdot\boldsymbol{n}, v\big\rangle_E + \big\langle\boldsymbol{\tau}\cdot\boldsymbol{n}, u\big\rangle_E\big] \\ & - \sum_{E\in\mathcal{E}_{int}} \frac{\gamma}{h_E}\big\langle[\![u]\!], [\![v]\!]\big\rangle_E - \sum_{E\in\mathcal{E}_D} \frac{\gamma}{h_E}\big\langle u, v\big\rangle_E \end{aligned}$$

and

$$\mathcal{L}(v, \boldsymbol{\tau}) := \big(-f, v\big)_\Omega - \big(g, v\big)_{\Gamma_N} + \sum_{E\in\mathcal{E}_D} \big\langle\boldsymbol{\tau}\cdot\boldsymbol{n}, u_0\big\rangle_E - \sum_{E\in\mathcal{E}_D} \frac{\gamma}{h_E}\big\langle u_0, v\big\rangle_E.$$

By the derivation of the variational form it is clear that the proposed method is consistent, i.e., the solution to (2.2) is also the solution to the variational problem (2.9).

The energy norm of the variational problem is

$$\begin{aligned} |\!|\!| v, \boldsymbol{\tau} |\!|\!|^2 := & \sum_{T\in\mathcal{T}_h} \Big[\|\boldsymbol{\tau}\|^2_{L^2(T)} + \|\nabla v\|^2_{L^2(T)}\Big] \\ & + \sum_{E\in\mathcal{E}_{\text{int}}} \frac{1}{h_E}\|[\![v]\!]\|^2_{L^2(E)} + \sum_{E\in\mathcal{E}_D} \frac{1}{h_E}\|v\|^2_{L^2(E)}. \end{aligned}$$

Note that the energy norm is mesh dependent. In order to prove the method to be continuous and elliptic in the energy norm we need the following estimate (which is easily proved by scaling).

LEMMA 2.1. *These exists a positive constant C_I, such that*

$$h_E\|\boldsymbol{\tau}\|^2_{L^2(\partial T)} \le C_I\|\boldsymbol{\tau}\|^2_{L^2(T)} \quad \forall \boldsymbol{\tau} \in W_h \ \textit{and} \ \forall T \in \mathcal{T}_h.$$

With Lemma 2.1 it is straightforward to show that the proposed bilinear form $a(\cdot, \cdot; \cdot, \cdot)$ and the linear functional $\mathcal{L}(\cdot, \cdot)$ are continuous in the energy norm $|\!|\!|\cdot, \cdot|\!|\!|$.

ETNA
Kent State University
etna@mcs.kent.edu

3. The stability and the a priori error estimates. In this section we show that the method is stable for all positive values of the stability parameter γ.

THEOREM 3.1. *There exists a positive constant C, such that*

$$\sup_{(v,\boldsymbol{\tau})\in V_h\times W_h} \frac{a(u,\boldsymbol{\sigma};v,\boldsymbol{\tau})}{|||v,\boldsymbol{\tau}|||} \geq C|||u,\boldsymbol{\sigma}||| \quad \forall (u,\boldsymbol{\sigma})\in V_h\times W_h. \tag{3.1}$$

Proof. First, we note that

$$a(u,\boldsymbol{\sigma};-u,\boldsymbol{\sigma}) = \sum_{T\in\mathcal{T}_h}\|\boldsymbol{\sigma}\|^2_{L^2(T)} + \sum_{E\in\mathcal{E}_{\text{int}}}\frac{\gamma}{h_E}\|[\![u]\!]\|^2_{L^2(E)} + \sum_{E\in\mathcal{E}_D}\frac{\gamma}{h_E}\|u\|^2_{L^2(E)}. \tag{3.2}$$

Next, we choose $\boldsymbol{\kappa}\in W_h$, such that $\boldsymbol{\kappa}=\nabla u$, which yields

$$\big(\boldsymbol{\kappa},\nabla u\big)_T = \|\nabla u\|^2_{L^2(T)} \quad \text{and} \quad \|\boldsymbol{\kappa}\|_{L^2(T)} \leq \|\nabla u\|_{L^2(T)}. \tag{3.3}$$

Then by the Schwarz inequality we get

$$\begin{aligned}
a(u,\boldsymbol{\sigma};0,-\boldsymbol{\kappa}) &= \sum_{T\in\mathcal{T}_h}\big[-\big(\boldsymbol{\sigma},\boldsymbol{\kappa}\big)_T + \big(\nabla u,\boldsymbol{\kappa}\big)_T\big] - \sum_{E\in\mathcal{E}_{\text{int}}}\big\langle\{\boldsymbol{\kappa}\cdot\boldsymbol{n}\},[\![u]\!]\big\rangle_E \\
&\quad - \sum_{E\in\mathcal{E}_D}\big\langle\boldsymbol{\kappa}\cdot\boldsymbol{n},u\big\rangle_E \\
&\geq \sum_{T\in\mathcal{T}_h}\Big[\|\nabla u\|^2_{L^2(T)} - \|\boldsymbol{\sigma}\|_{L^2(T)}\|\boldsymbol{\kappa}\|_{L^2(T)}\Big] \\
&\quad - \sum_{E\in\mathcal{E}_{\text{int}}}\frac{1}{2}\Big[h_E^{1/2}\|\boldsymbol{\kappa}_1\cdot\boldsymbol{n}_1\|_{L^2(E)}h_E^{-1/2}\|[\![u]\!]\|_{L^2(E)} \\
&\qquad + h_E^{1/2}\|\boldsymbol{\kappa}_2\cdot\boldsymbol{n}_1\|_{L^2(E)}h_E^{-1/2}\|[\![u]\!]\|_{L^2(E)}\Big] \\
&\quad - \sum_{E\in\mathcal{E}_D} h_E^{1/2}\|\boldsymbol{\kappa}\cdot\boldsymbol{n}\|_{L^2(E)}h_E^{-1/2}\|[\![u]\!]\|_{L^2(E)}.
\end{aligned}$$

For $\delta>0$, Lemma 2.1, (3.3) and Young's inequality give

$$\begin{aligned}
a(u,\boldsymbol{\sigma};0,-\boldsymbol{\kappa}) &\geq \sum_{T\in\mathcal{T}_h}\|\nabla u\|^2_{L^2(T)} - \frac{1}{2\delta}\|\boldsymbol{\sigma}\|^2_{L^2(\Omega)} - \frac{\delta}{2}\sum_{T\in\mathcal{T}_h}\|\nabla u\|^2_{L^2(T)} \\
&\quad - \frac{C_I\delta}{2}\sum_{T\in\mathcal{T}_h}\|\nabla u\|^2_{L^2(T)} - \frac{1}{2\delta}\sum_{E\in\mathcal{E}_{\text{int}}}\frac{1}{h_E}\|[\![u]\!]\|^2_{L^2(E)} \\
&\quad - \frac{1}{2\delta}\sum_{E\in\mathcal{E}_D}\frac{1}{h_E}\|u\|^2_{L^2(E)} \\
&= \Big(1-\frac{\delta}{2}\big(1+C_I\big)\Big)\sum_{T\in\mathcal{T}_h}\|\nabla u\|^2_{L^2(T)} - \frac{1}{2\delta}\|\boldsymbol{\sigma}\|^2_{L^2(\Omega)} \\
&\quad - \frac{1}{2\delta}\sum_{E\in\mathcal{E}_{\text{int}}}\frac{1}{h_E}\|[\![u]\!]\|^2_{L^2(E)} - \frac{1}{2\delta}\sum_{E\in\mathcal{E}_D}\frac{1}{h_E}\|u\|^2_{L^2(E)}.
\end{aligned}$$

Choosing $\delta < 2/(1+C_I)$ yields

$$\begin{aligned}
a(u,\boldsymbol{\sigma};0,-\boldsymbol{\kappa}) &\geq -C_1\|\boldsymbol{\sigma}\|^2_{L^2(\Omega)} + C_2\sum_{T\in\mathcal{T}_h}\|\nabla u\|^2_{L^2(T)} \\
&\quad - C_1\sum_{E\in\mathcal{E}_{\text{int}}}\frac{1}{h_E}\|[\![u]\!]\|^2_{L^2(E)} - C_1\sum_{E\in\mathcal{E}_D}\frac{1}{h_E}\|u\|^2_{L^2(E)},
\end{aligned} \tag{3.4}$$

ETNA
Kent State University
etna@mcs.kent.edu

with positive constants C_1 and C_2 independent of the stability parameter γ. Using the linearity and combining (3.2) and (3.4) we get

$$\begin{aligned} a(u,\boldsymbol{\sigma},-u,\boldsymbol{\sigma}-\epsilon\boldsymbol{\kappa}) &\geq (1-\epsilon C_1)\|\boldsymbol{\sigma}\|^2_{L^2(\Omega)} + \epsilon C_2 \sum_{T\in\mathcal{T}_h} \|\nabla u\|^2_{L^2(T)} \\ &+ (\gamma-\epsilon C_1)\sum_{E\in\mathcal{E}_{\text{int}}} \frac{1}{h_E}\|[\![u]\!]\|^2_{L^2(E)} + (\gamma-\epsilon C_1)\sum_{E\in\mathcal{E}_D}\frac{1}{h_E}\|u\|^2_{L^2(E)}. \end{aligned} \tag{3.5}$$

Choosing the parameter ϵ, such that

$$\epsilon > 0, \quad \epsilon < \frac{1}{C_1} \quad \text{and} \quad \epsilon < \frac{\gamma}{C_1},$$

the inequality (3.5) gives

$$a(u,\boldsymbol{\sigma},-u,\boldsymbol{\sigma}-\epsilon\boldsymbol{\kappa}) \geq C_3 |||u,\boldsymbol{\sigma}|||^2, \tag{3.6}$$

with a constant $C_3 > 0$. By the definition of $\boldsymbol{\kappa}$ it is clear that

$$|||-u,\boldsymbol{\sigma}-\epsilon\boldsymbol{\kappa}||| \leq C_4 |||u,\boldsymbol{\sigma}|||. \tag{3.7}$$

Substituting (3.6) and (3.7) into the left hand side of (3.1) proves the claim. ◻

From the stability and consistency we directly get the a priori estimate. The lower bound $s > 3/2$ ensures that $\boldsymbol{\sigma}\cdot\boldsymbol{n} \in L^2(E)$ for all $E \in \mathcal{E}_{\text{int}} \cup \mathcal{E}_{\partial\Omega}$.

THEOREM 3.2. *For $u \in H^s(\Omega)$, with $3/2 < s \leq k+1$ it holds*

$$|||u-u_h,\boldsymbol{\sigma}-\boldsymbol{\sigma}_h||| \leq Ch^{s-1}\|u\|_{H^s(\Omega)}.$$

From above we see that the difference of this method compared to the standard discontinuous Galerkin method is that the lower bound (i.e. zero) is readily available. Let us discuss the implementation of the method a little further. The form of the discrete equations is the following

$$\begin{bmatrix} \mathbf{A} & \mathbf{B} \\ \mathbf{B}^T & \mathbf{C} \end{bmatrix} \begin{bmatrix} \boldsymbol{\Sigma} \\ \mathbf{U} \end{bmatrix} = \begin{bmatrix} \mathbf{0} \\ \mathbf{F} \end{bmatrix},$$

where $\boldsymbol{\Sigma}$ and $\mathbf{U}$ are the degrees of freedom for $\boldsymbol{\sigma}_h$ and u_h, respectively. Eliminating $\boldsymbol{\Sigma}$, yields the system of equations for $\mathbf{U}$:

$$\big(\mathbf{C} - \mathbf{B}^T\mathbf{A}^{-1}\mathbf{B}\big)\mathbf{U} = \mathbf{F}. \tag{3.8}$$

Since the matrix $\mathbf{A}$ corresponds to the part $\sum_{T\in\mathcal{T}_h}\big(\boldsymbol{\sigma},\boldsymbol{\tau}\big)_T$ in the bilinear form it is inverted element by element (i.e. condensed) and the cost of this is negligible. For triangular elements the situation is even simpler. An orthogonalization of the basis functions on the reference element gives orthogonal functions on the real element and in this case $\mathbf{A}$ is diagonal. Further, it should be noted that the stability of the method implies that the matrix in (3.8) is positively definite. The conclusion is hence, that this method is implemented very similarly to the standard discontinuous Galerkin method, but with the advantage that the stability is ensured for all values of the stability parameter.

4. The a posteriori error estimate. In this section we introduce and prove the following a posteriori error estimate for the method.

THEOREM 4.1. *There exists a positive constant C, such that*

$$|||u-u_h,\boldsymbol{\sigma}-\boldsymbol{\sigma}_h||| \le C\Big(\sum_{T\in\mathcal{T}_h}\eta_T^2\Big)^{1/2},$$

in which

$$\begin{aligned}\eta_T^2 := {} & h_T^2\|\nabla\cdot\boldsymbol{\sigma}_h+f\|^2_{L^2(T)}+\|\boldsymbol{\sigma}_h-\nabla u_h\|^2_{L^2(T)}\\ & + h_E\,\|[\![\boldsymbol{\sigma}_h\cdot\boldsymbol{n}]\!]\|^2_{L^2(\partial T\cap\mathcal{E}_{int})}+\frac{1}{h_E}\|[\![u_h]\!]\|^2_{L^2(\partial T\cap\mathcal{E}_{int})}\\ & + h_E\|\boldsymbol{\sigma}\cdot\boldsymbol{n}-g\|_{L^2(\partial T\cap\mathcal{E}_N)}+\frac{1}{h_E}\|u_h-u_0\|^2_{L^2(\partial T\cap\mathcal{E}_D)}.\end{aligned}$$

In the proof of Theorem 4.1 we need the following Helmholtz decomposition, cf. [1, 4, 6].

THEOREM 4.2. *For every vector $\boldsymbol{\tau}\in[L^2(\Omega)]^2$, with $\boldsymbol{\tau}\cdot\boldsymbol{n}=g$ on Γ_N, there exists $\psi\in H^1(\Omega)$, with $\psi_{|\Gamma_D}=0$, and $q\in H^1(\Omega)/\mathbb{R}$, with $\mathbf{curl}\,q\cdot\boldsymbol{n}_{|\Gamma_N}=0$, such that*

$$\boldsymbol{\tau}=\nabla\psi+\mathbf{curl}\,q \quad \textit{and} \quad \|\boldsymbol{\tau}\|^2_{L^2(\Omega)}=\|\nabla\psi\|^2_{L^2(\Omega)}+\|\mathbf{curl}\,q\|^2_{L^2(\Omega)}\,.$$

The **curl** operator, used in the Theorem 4.2, is defined as

$$\mathbf{curl}\,v := \begin{bmatrix} -\frac{\partial v}{\partial x_2}\\ \frac{\partial v}{\partial x_1}\end{bmatrix},$$

when $v\in H^1(\Omega)$ and $\Omega\subset\mathbb{R}^2$. We define the tangent to an edge $E\in\mathcal{E}_{\text{int}}\cup\mathcal{E}_{\partial\Omega}$ by

$$\boldsymbol{t} := \begin{bmatrix} t_1\\ t_2\end{bmatrix} = \begin{bmatrix} -n_2\\ n_1\end{bmatrix},$$

in which $\boldsymbol{n}=(n_1,n_2)$ denotes the outer normal vector of the edge E. The operator $\nabla\times$ is defined by

$$\nabla\times\begin{bmatrix} v_1\\ v_2\end{bmatrix} := \frac{\partial v_2}{\partial x_1}-\frac{\partial v_1}{\partial x_2}.$$

Proof of Theorem 4.1. Since the exact solution is continuous and fulfils the boundary conditions, we get

$$\begin{aligned}|||u-u_h,\boldsymbol{\sigma}-\boldsymbol{\sigma}_h|||^2 = {} & \|\boldsymbol{\sigma}-\boldsymbol{\sigma}_h\|^2_{L^2(\Omega)}+\sum_{T\in\mathcal{T}_h}\|\nabla u-\nabla u_h\|^2_{L^2(T)}\\ & +\sum_{E\in\mathcal{E}_{\text{int}}}\frac{1}{h_E}\|[\![u_h]\!]\|^2_{L^2(E)}+\sum_{E\in\mathcal{E}_D}\frac{1}{h_E}\|u_0-u_h\|^2_{L^2(E)}.\end{aligned}\tag{4.1}$$

The two last terms of (4.1) already belong to the indicator η_T and therefore we only need to estimate the first two terms. We begin with the first term. The definition of the norm and Theorem 4.2 yield

$$\begin{aligned}\|\boldsymbol{\sigma}-\boldsymbol{\sigma}_h\|_{L^2(\Omega)} = {} & \sup_{\boldsymbol{\tau}\in[L^2(\Omega)]^2}\frac{\big(\boldsymbol{\sigma}-\boldsymbol{\sigma}_h,\boldsymbol{\tau}\big)_\Omega}{\|\boldsymbol{\tau}\|_{L^2(\Omega)}}\\ & \le \sup_{\psi}\frac{\big(\boldsymbol{\sigma}-\boldsymbol{\sigma}_h,\nabla\psi\big)_\Omega}{\|\nabla\psi\|_{L^2(\Omega)}}+\sup_{q}\frac{\big(\boldsymbol{\sigma}-\boldsymbol{\sigma}_h,\mathbf{curl}\,q\big)_\Omega}{\|\nabla q\|_{L^2(\Omega)}}.\end{aligned}\tag{4.2}$$

Next we turn our attention to the first term in (4.2). Since $\psi \in H^1(\Omega)$ and $\psi_{|\Gamma_D} = 0$, there exists a continuous and piecewise linear Clément interpolation $I_h\psi$ that vanishes on the boundary Γ_D and fulfils

$$\sum_{T\in\mathcal{T}_h} h_T^{-1} \|\psi - I_h\psi\|_{L^2(T)} + \sum_{E\in\mathcal{E}_{\text{int}}\cup\mathcal{E}_N} h_E^{-1/2} \|\psi - I_h\psi\|_{L^2(E)} \le C\|\nabla\psi\|_{L^2(\Omega)}. \tag{4.3}$$

The bilinear form gives us

$$0 = a(u-u_h, \boldsymbol{\sigma}-\boldsymbol{\sigma}_h; I_h\psi, 0) = \sum_{T\in\mathcal{T}_h} \left(\boldsymbol{\sigma}-\boldsymbol{\sigma}_h, \nabla I_h\psi\right)_T. \tag{4.4}$$

The orthogonality above yields

$$\begin{aligned}
&\left(\boldsymbol{\sigma}-\boldsymbol{\sigma}_h, \nabla\psi\right)_\Omega = \sum_{T\in\mathcal{T}_h} \left(\boldsymbol{\sigma}-\boldsymbol{\sigma}_h, \nabla(\psi - I_h\psi)\right)_T \\
&= \sum_{T\in\mathcal{T}_h} \left[-\left(\nabla\cdot(\boldsymbol{\sigma}-\boldsymbol{\sigma}_h), \psi - I_h\psi\right)_T + \left((\boldsymbol{\sigma}-\boldsymbol{\sigma}_h)\cdot\boldsymbol{n}, \psi - I_h\psi\right)_{\partial T}\right] \\
&= \sum_{T\in\mathcal{T}_h} \left(\nabla\cdot\boldsymbol{\sigma}_h + f, \psi - I_h\psi\right)_T + \sum_{E\in\mathcal{E}_{\text{int}}} \left([\![(\boldsymbol{\sigma}-\boldsymbol{\sigma}_h)\cdot\boldsymbol{n}]\!], \{\psi - I_h\psi\}\right)_E \\
&\quad + \sum_{E\in\mathcal{E}_N} \left\langle g - \boldsymbol{\sigma}_h\cdot\boldsymbol{n}, \psi - I_h\psi\right\rangle_E.
\end{aligned}$$

Applying the Schwarz inequality and (4.3) gives

$$\begin{aligned}
&\left(\boldsymbol{\sigma}-\boldsymbol{\sigma}_h, \nabla\psi\right)_\Omega \\
&\le \sum_{T\in\mathcal{T}_h} h_T \|\nabla\cdot\sigma_h + f\|_{L^2(T)}\, h_T^{-1}\|\psi - I_h\psi\|_{L^2(T)} \\
&\quad + \sum_{E\in\mathcal{E}_{\text{int}}} h_E^{1/2} \|[\![\boldsymbol{\sigma}_h\cdot\boldsymbol{n}]\!]\|_{L^2(E)}\, h_E^{-1/2} \|\psi - I_h\psi\|_{L^2(E)} \\
&\quad + \sum_{E\in\mathcal{E}_N} h_E^{1/2} \|g - \boldsymbol{\sigma}_h\cdot\boldsymbol{n}\|_{L^2(E)}\, h_E^{-1/2} \|\psi - I_h\psi\|_{L^2(E)} \\
&\le C\Bigg\{ \sum_{T\in\mathcal{T}_h} h_T^2 \|\nabla\cdot\boldsymbol{\sigma}_h + f\|_{L^2(T)}^2 + \sum_{E\in\mathcal{E}_{\text{int}}} h_E \|[\![\boldsymbol{\sigma}_h\cdot\boldsymbol{n}]\!]\|_{L^2(E)}^2 \\
&\quad + \sum_{E\in\mathcal{E}_N} h_E \|g - \boldsymbol{\sigma}_h\cdot\boldsymbol{n}\|_{L^2(E)}^2 \Bigg\}^{1/2} \|\nabla\psi\|_{L^2(\Omega)}.
\end{aligned}$$

Now, the first term in (4.2) is bounded by the indicator η_T.

Next, we consider the second term. For the function $q \in H^1(\Omega)/\mathbb{R}$ we construct a piecewise linear interpolate $\pi_h q$ in the following way. Since $\mathbf{curl}\, q\cdot\boldsymbol{n}_{|\Gamma_N} = 0$, it follows that $q_{|\Gamma_N}$ is a constant. On Γ_N we thus assign this constant value to $\pi_h q$. For all other vertices we use the Clément construction. The following interpolation estimate holds.

$$\begin{aligned}
\sum_{T\in\mathcal{T}_h} h_T^{-1} \|q - \pi_h q\|_{L^2(T)} &+ \sum_{E\in\mathcal{E}_{\text{int}}\cup\mathcal{E}_D} h_E^{-1/2} \|q - \pi_h q\|_{L^2(E)} \\
&+ \|\mathbf{curl}(q - \pi_h q)\|_{L^2(\Omega)} \le C\|\mathbf{curl}\, q\|_{L^2(\Omega)}.
\end{aligned} \tag{4.5}$$

Integrating by parts gives us

$$0 = a(u - u_h, \boldsymbol{\sigma} - \boldsymbol{\sigma}_h; 0, \mathbf{curl}\, \pi_h q) = \sum_{T \in \mathcal{T}_h} \big(\boldsymbol{\sigma} - \boldsymbol{\sigma}_h, \mathbf{curl}\, \pi_h q\big)_T,$$

which leads to

$$\begin{aligned}
\big(\boldsymbol{\sigma} - \boldsymbol{\sigma}_h, \mathbf{curl}\, q\big)_\Omega &= \sum_{T \in \mathcal{T}_h} \big(\nabla u - \boldsymbol{\sigma}_h, \mathbf{curl}(q - \pi_h q)\big)_T \\
&= \sum_{T \in \mathcal{T}_h} \big[\big(\nabla u - \nabla u_h, \mathbf{curl}(q - \pi_h q)\big)_T + \big(\nabla u_h - \boldsymbol{\sigma}_h, \mathbf{curl}(q - \pi_h q)\big)_T\big] \\
&=: R_1 + R_2.
\end{aligned}$$

Integrating by parts and using the result $\nabla \times \nabla v = 0$ in T we get

$$\begin{aligned}
R_1 &= \sum_{T \in \mathcal{T}_h} \big[-\big(\nabla \times \nabla(u - u_h), q - \pi_h q\big)_T + \big(\nabla(u - u_h) \cdot \boldsymbol{t}, q - \pi_h q\big)_{\partial T}\big] \\
&= \sum_{E \in \mathcal{E}_{\text{int}}} \big\langle [\![\nabla(u - u_h) \cdot \boldsymbol{t}]\!], q - \pi_h q\big\rangle_E + \sum_{E \in \mathcal{E}_{\partial\Omega}} \big\langle \nabla(u - u_h) \cdot \boldsymbol{t}, q - \pi_h q\big\rangle_E \\
&= - \sum_{E \in \mathcal{E}_{\text{int}}} \big\langle [\![\nabla u_h \cdot \boldsymbol{t}]\!], q - \pi_h q\big\rangle_E + \sum_{E \in \mathcal{E}_{\partial\Omega}} \big\langle \nabla(u - u_h) \cdot \boldsymbol{t}, q - \pi_h q\big\rangle_E \\
&=: S_1 + S_2.
\end{aligned}$$

The Schwarz inequality for sums and the estimate (4.5) lead to

$$\begin{aligned}
S_1 &\leq \Big(\sum_{E \in \mathcal{E}_{\text{int}}} h_E \, \|[\![\nabla u_h \cdot \boldsymbol{t}]\!]\|^2_{L^2(E)}\Big)^{1/2} \Big(\sum_{E \in \mathcal{E}_{\text{int}}} \frac{1}{h_E} \|q - \pi_h q\|^2_{L^2(E)}\Big)^{1/2} \\
&\leq C \Big(\sum_{E \in \mathcal{E}_{\text{int}}} \frac{1}{h_E} \|[\![u - u_h]\!]\|^2_{L^2(E)}\Big)^{1/2} \|\mathbf{curl}\, q\|_{L^2(\Omega)}.
\end{aligned} \tag{4.6}$$

In the previous bound, we have also used the inverse inequality

$$\|[\![\nabla u_h \cdot \boldsymbol{t}]\!]\|_{L^2(E)} \leq C \frac{1}{h_E} \|[\![u_h]\!]\|_{L^2(E)}.$$

By (4.6), S_1 is bounded by the indicator η_T. Since $q - \pi_h q = 0$ on Γ_N, (4.5) gives

$$S_2 \leq C \left(\sum_{E \in \mathcal{E}_D} \frac{1}{h_E} \|u_h - u_0\|^2_{L^2(E)}\right) \|\mathbf{curl}\, q\|_{L^2(\Omega)}, \tag{4.7}$$

since both q and $\pi_h q$ vanish on Γ_N. Combining (4.6) and (4.7) shows that the term R_1 is bounded by the indicator η_T. The Schwarz inequality for sums yields

$$\begin{aligned}
R_2 &\leq C \Big(\sum_{T \in \mathcal{T}_h} \|\nabla u_h - \boldsymbol{\sigma}_h\|^2_{L^2(T)}\Big)^{1/2} \Big(\sum_{T \in \mathcal{T}_h} \|\mathbf{curl}(q - \pi_h q)\|^2_{L^2(T)}\Big)^{1/2} \\
&\leq C \Big(\sum_{T \in \mathcal{T}_h} \|\nabla u_h - \boldsymbol{\sigma}_h\|^2_{L^2(T)}\Big)^{1/2} \|\mathbf{curl}\, q\|^2_{L^2(\Omega)}.
\end{aligned}$$

Now, we have proved that

$$\|\boldsymbol{\sigma} - \boldsymbol{\sigma}_h\|^2_{L^2(\Omega)} \leq C \sum_{T \in \mathcal{T}_h} \eta_T^2, \tag{4.8}$$

ETNA
Kent State University
etna@mcs.kent.edu

and we still need to bound the second term in (4.1). (4.8) and the definition of η_T lead to

$$\begin{aligned}\sum_{T\in\mathcal{T}_h}\|\nabla(u-u_h)\|^2_{L^2(T)} &= \sum_{T\in\mathcal{T}_h}\|\boldsymbol{\sigma}-\nabla u_h\|^2_{L^2(T)}\\ &\le 2\sum_{T\in\mathcal{T}_h}\left[\|\boldsymbol{\sigma}-\boldsymbol{\sigma}_h\|^2_{L^2(T)}+\|\boldsymbol{\sigma}_h-\nabla u_h\|^2_{L^2(T)}\right]\le C\sum_{T\in\mathcal{T}_h}\eta_T^2.\end{aligned}\tag{4.9}$$

Combining (4.1), (4.8), and (4.9) completes the proof. $\square$

Next we give the lower bound estimate. The claim follows from standard techniques, see [9], and the proof is omitted here.

THEOREM 4.3. *There exists a positive constant C, such that*

$$\begin{aligned}\eta_T^2 \le C\Big(&|u-u_h|^2_{H^1(\omega_T)}+\|\boldsymbol{\sigma}-\boldsymbol{\sigma}_h\|^2_{L^2(\omega_T)}+h_T^2\|f-f_h\|^2_{L^2(\omega_T)}+\frac{1}{h_T}\|u-u_h\|^2_{L^2(\partial T)}\\ &+h_T\|g-g_h\|^2_{L^2(\partial T\cap\mathcal{E}_N)}+\frac{1}{h_T}\|u_0-u_{0,h}\|^2_{L^2(\partial T\cap\mathcal{E}_D)}\Big).\end{aligned}$$

Above we denote with ω_T the union of T and all the elements sharing an edge with T. With f_h, g_h and $u_{0,h}$ we denote the projections of the given data to the discrete space.

5. Numerical results. In this section we investigate the numerical performance of the Nitsche method. We show that the Nitsche method has the optimal convergence rate with respect to the mesh size h. After that we test the adaptive refinement based on the a posteriori error estimate. In all the computations, if not otherwise stated, the stability parameter is set to $\gamma = 1$. A choice which would produce an unstable Nitsche method for the non-mixed problem.

For simplicity we choose the unit square as the computational domain; $\Omega = (0,1)\times(0,1)$. To have a problem with typical corner singularities we choose our exact solution to be, in polar coordinates,

$$u(r,\theta) = r^\beta \sin(\beta\theta),$$

with the parameter $\beta > 0$. With β we can control the regularity of the solution, namely

$$u \in H^{\beta+1-\delta}(\Omega),$$

for all $\delta > 0$. The chosen exact solution u is harmonic ($f = 0$) and we compute the boundary conditions from it, i.e., we define

$$u_0 = u(r,\theta) \quad\text{and}\quad g = \frac{\partial u(r,\theta)}{\partial n} \text{ on } \partial\Omega.$$

Our model problem is:

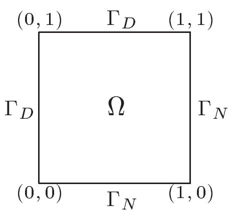

$$\begin{aligned}\boldsymbol{\sigma}-\nabla u &= 0 &&\text{on } \partial\Omega\\ \nabla\cdot\boldsymbol{\sigma} &= 0 &&\text{on } \partial\Omega\\ u &= u_0 &&\text{on } \Gamma_D\\ \boldsymbol{\sigma}\cdot\boldsymbol{n} &= g &&\text{on } \Gamma_N\end{aligned}$$

The convergence results are computed with parameter values $\beta = 0.7$, 1.3 and 2.3. With this choice the solution belongs to $u \in H^{1.7-\delta}(\Omega)$, $H^{2.3-\delta}(\Omega)$ and $H^{3.3-\delta}(\Omega)$, respectively.

ETNA
Kent State University
etna@mcs.kent.edu

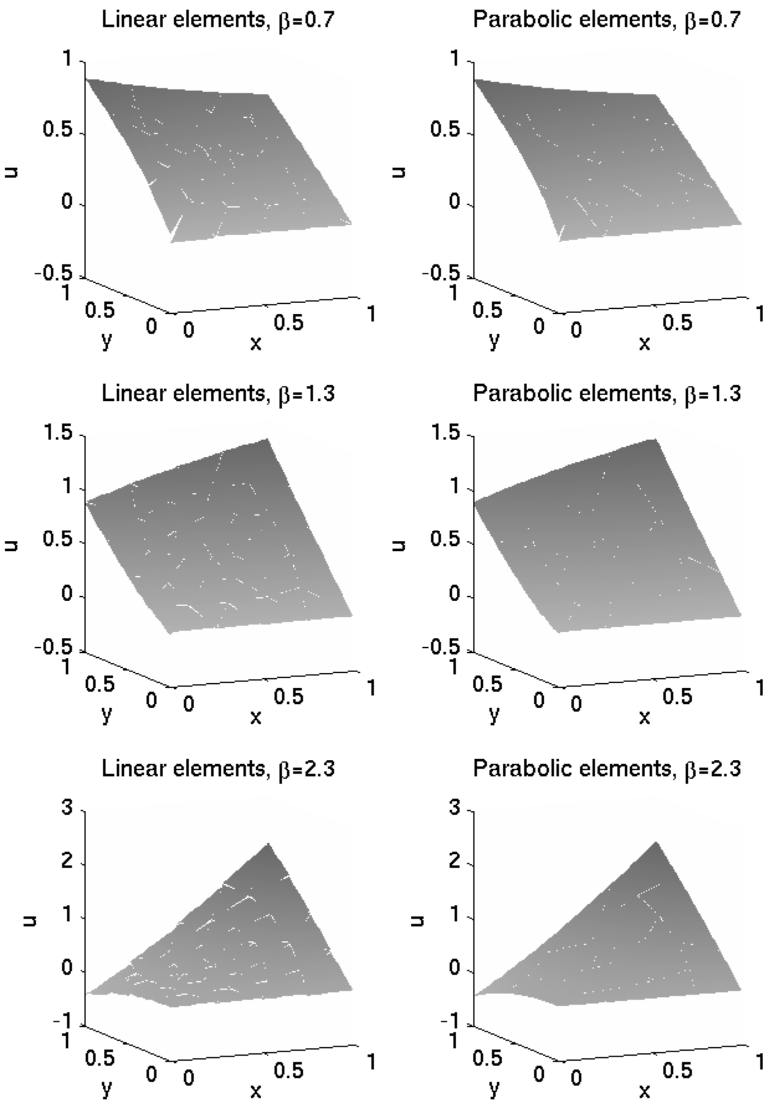

FIG. 5.1. *Solutions to the model problem with different values of the parameter β. On the left are the solutions with linear elements and on the right with parabolic elements. From top to bottom β has values* 0.7, 1.3 *and* 2.3. *The mesh is of size* $h = 0.25$.

Figure 5.1 shows the solutions for the chosen values of β with both linear and parabolic elements on a mesh of size $h = 0.25$.

In Figure 5.2 we show the convergence of the error in the energy norm $|||\cdot,\cdot|||$ for both linear and parabolic elements, with different values of β and using a uniform mesh refinement. Both methods perform as expected by the analytical results. Note that the linear elements

ETNA
Kent State University
etna@mcs.kent.edu

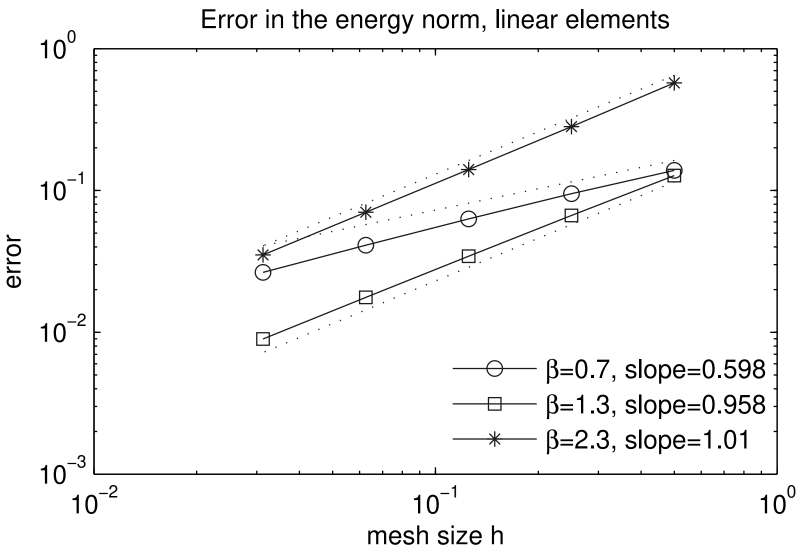

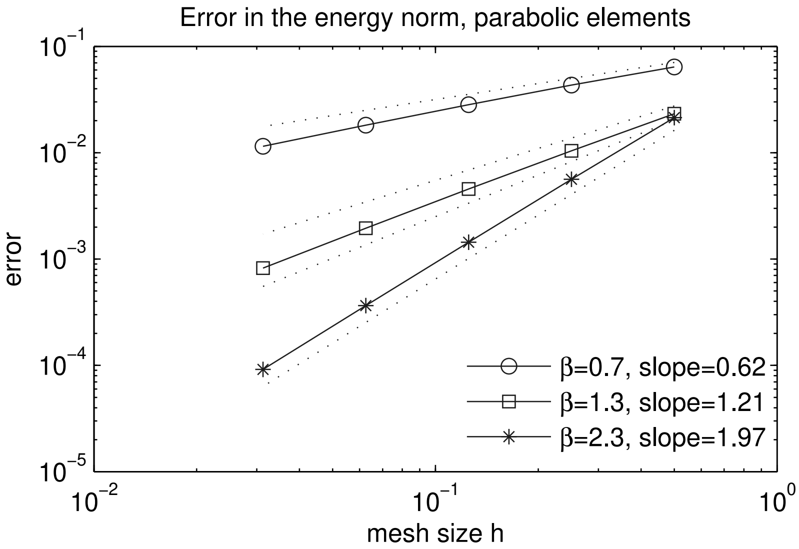

FIG. 5.2. *Convergence of the error in the energy norm in uniform mesh refinement for different values of β. The dotted lines are reference convergence rates of $Ch^{0.7}$, Ch, $Ch^{1.3}$ and Ch^2. The numerical values of the slopes are in the legends.*

cannot take advantage of the regularity beyond $u \in H^2(\Omega)$. The numerical values of the slopes are given in the legends of the figures.

Next we test the adaptive mesh refinement based on the a posteriori error distribution. On each step we refine the elements that have larger error than the average elementwise error. The elementwise errors and the average elementwise error are given by the a posteriori error

ETNA
Kent State University
etna@mcs.kent.edu

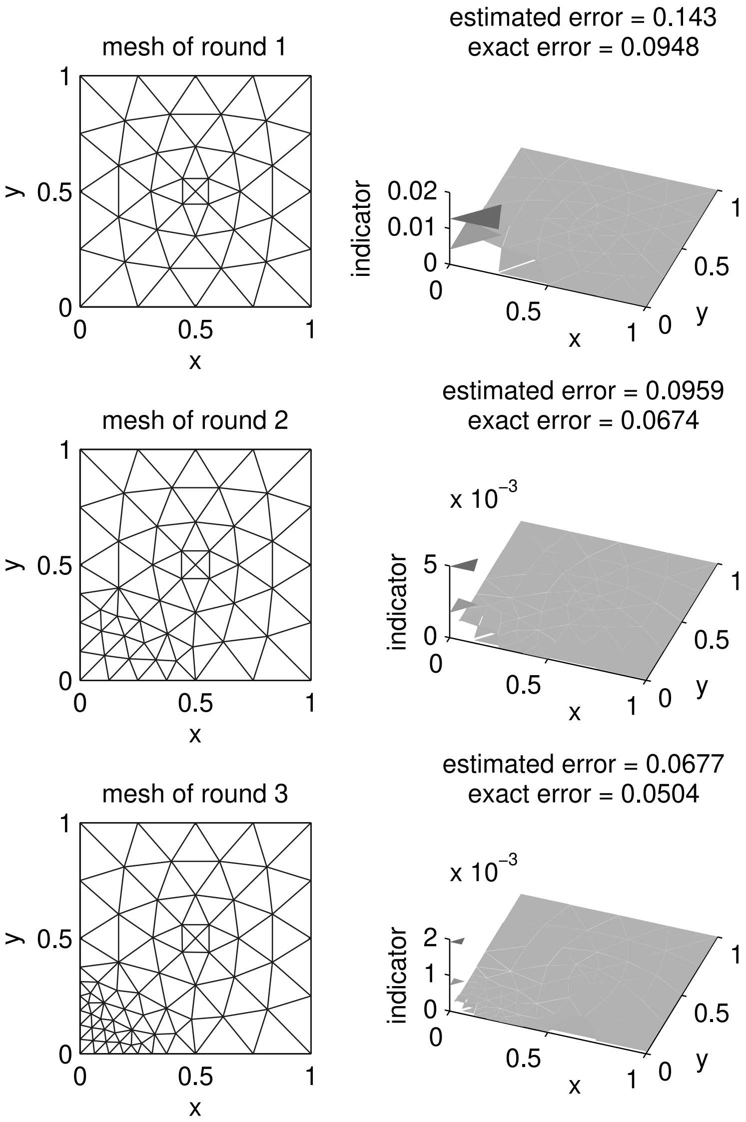

FIG. 5.3. *The first three meshes in the adaptive refinement with linear elements and $\beta = 0.7$. On the left the mesh and on the right the distribution of the a posteriori error. In the titles on the right we give the estimated and the exact error in the energy norm. Here the non-regularity at the origin dominates the error.*

estimator. Figure 5.3 shows the first three adaptive mesh refinements for linear elements with $\beta = 0.7$. The first mesh has the size $h = 0.25$. We see that the error indicator notices the singularity at the origin and refines there, but that the error at the origin is still dominant after two refinements. In Figure 5.4 is the same computation with parabolic elements. Again the singularity at the origin dominates the error.

ETNA
Kent State University
etna@mcs.kent.edu

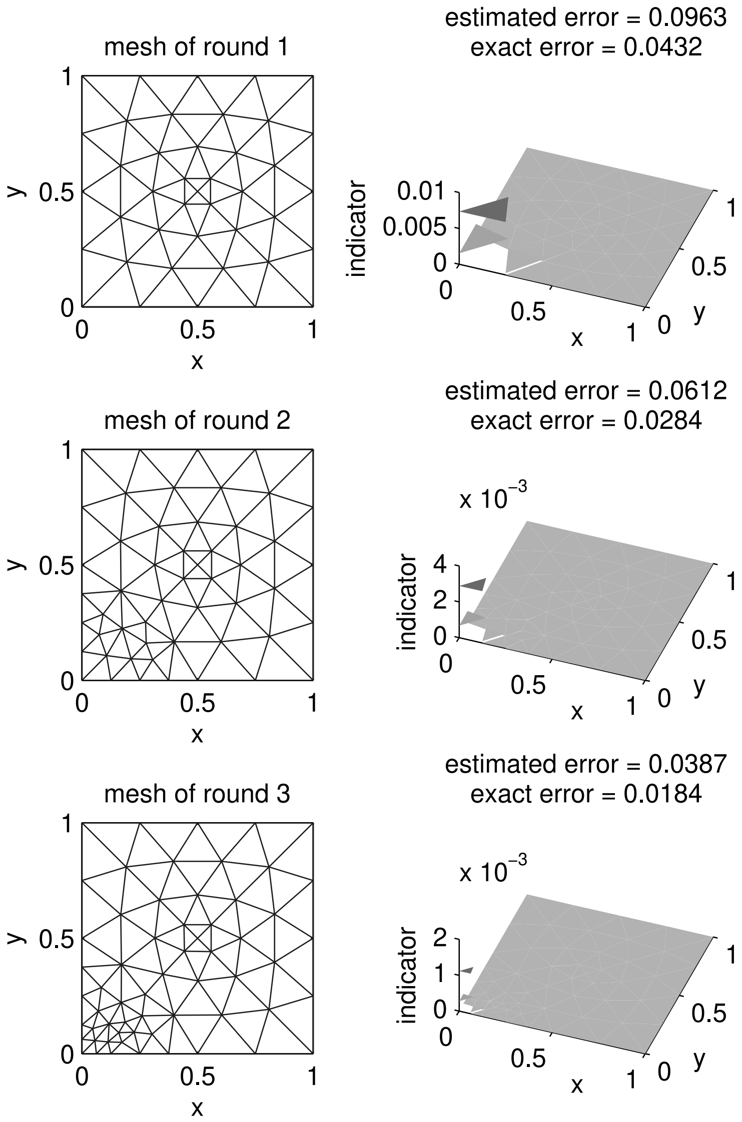

FIG. 5.4. *The first three meshes in the adaptive refinement with parabolic elements and $\beta = 0.7$. On the left the mesh and on the right the distribution of the a posteriori error. In the titles on the right we give the estimated and the exact error in the energy norm. Here the non-regularity at the origin dominates the error.*

Figure 5.5 shows three adaptive refinements for linear elements and $\beta = 2.3$. We see that the origin is not the dominant part here, instead the error indicator notices the large changes at the boundaries and refines there. In Figure 5.6 we show the mesh refinements for parabolic elements. Now the origin is again the dominant part of the error since the parabolic elements are able to capture the large but smooth changes at the boundaries with larger elements.

ETNA
Kent State University
etna@mcs.kent.edu

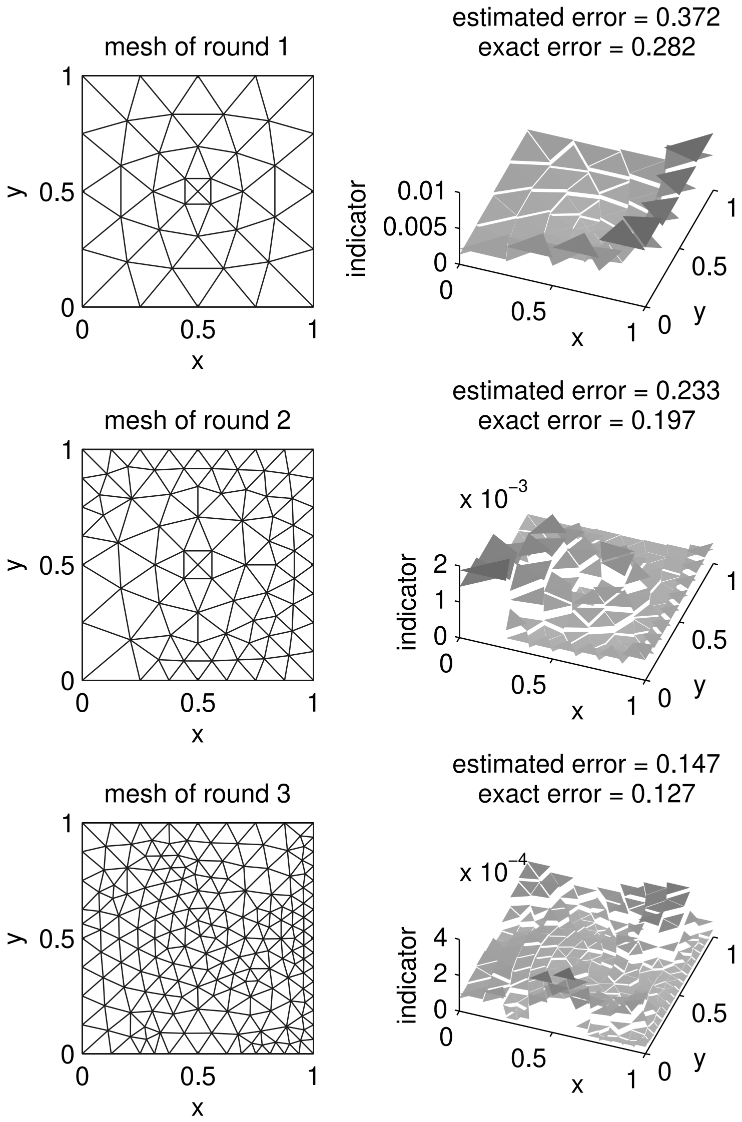

FIG. 5.5. *The first three meshes in the adaptive refinement with linear elements and $\beta = 2.3$. On the left the mesh and on the right the distribution of the a posteriori error. In the titles on the right we give the estimated and the exact error in the energy norm. Now, the large changes at the boundaries dominate the error.*

Notice also the scales of the error when comparing to Figure 5.5.

Figures 5.3–5.6 also show the estimated error and the exact error in the energy norm. We see that both diminish at the same speed, as predicted by the theory.

Acknowledgements. We would like to thank the anonymous referees for their careful reading of the manuscript and their suggestions for improvements. This paper was partly

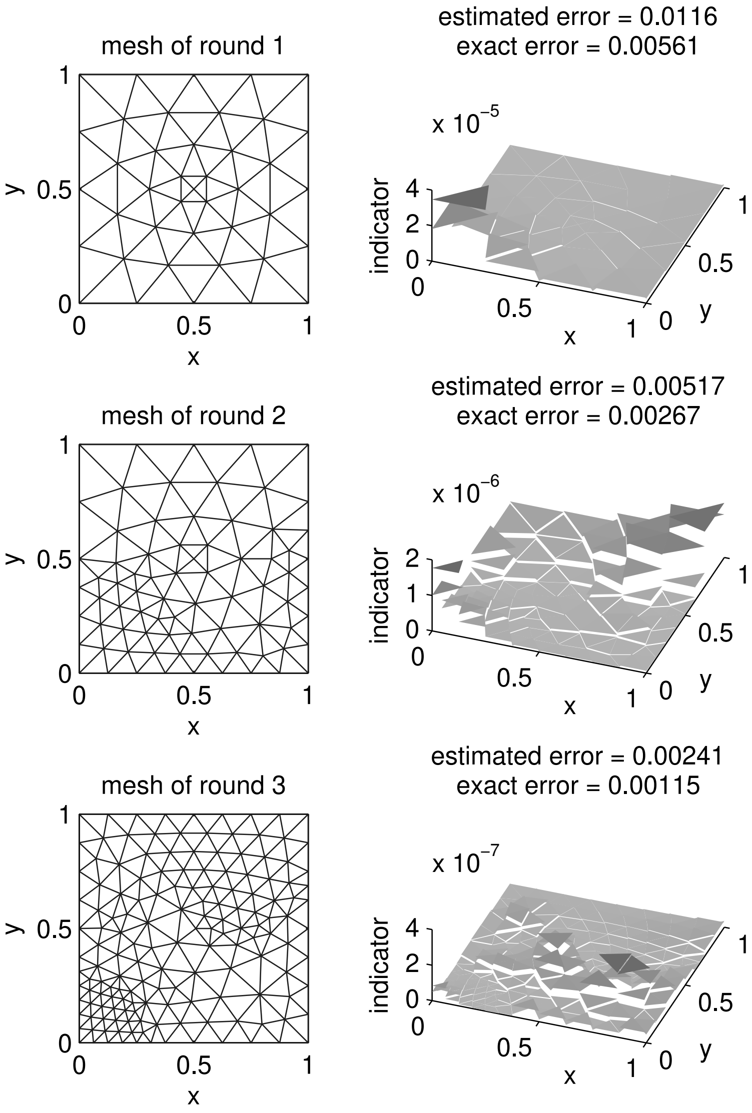

FIG. 5.6. *The first three meshes in the adaptive refinement with parabolic elements and $\beta = 2.3$. On the left the mesh and on the right the distribution of the a posteriori error. In the titles on the right we give the estimated and the exact error in the energy norm. Parabolic elements capture the large but smooth changes at the boundaries and the singularity at the origin dominates the error.*

written when the second author was visiting Laboratoire Jacques-Louis Lions, Université Pierre et Marie Curie and he would like to thank Prof. Vivette Girault for the kind invitation and the hospitality. The work has been supported by the Finnish National Graduate School in Engineering Mechanics and TEKES, The National Technology Agency of Finland (project KOMASI, decision number 210622).

REFERENCES

[1] A. ALONSO, *Error estimators for a mixed method*, Numer. Math., 74 (1976), pp. 385–395.

[2] F. BASSI AND S. REBAY, *High-order accurate discontinuous finite element solution of the 2D Euler equations*, J. Comput. Phys., 138 (1997), pp. 251–285.

[3] F. BREZZI, B. COCKBURN, L. MARINI, AND E. SÜLI, *Stabilization mechanism in discontinuous Galerkin finite element methods*, Comput. Methods Appl. Mech. Engrg., 195 (2006), pp. 3293–3310.

[4] E. DARI, R. DURÁN, C. PADRA, AND V. VAMPA, *A posteriori error estimators for nonconforming finite element methods*, M2AN Math. Model. Numer. Anal., 30 (1996), pp. 385–400.

[5] L. P. FRANCA AND R. STENBERG, *Error analysis of Galerkin least squares methods for the elasticity equations*, SIAM J. Numer. Anal., 28 (1991), pp. 1680–1697.

[6] V. GIRAULT AND P. RAVIART, *Finite Element Methods for Navier-Stokes Equations, Theory and Algorithms*, Springer-Verlag, Berlin, 1986.

[7] J. NITSCHE, *Über ein Variationsprinzip zur Lösung von Dirichlet-Problemen bei Verwendung von Teilräumen, die keinen Randbedingungen unterworfen sind*, Abh. Math. Sem. Univ. Hamburg, 36 (1970/71), pp. 9–15.

[8] R. STENBERG, *On some techniques for approximating boundary conditions in the finite element method*, J. Comput. Appl. Math., 63 (1995), pp. 139–148.

[9] R. VERFÜRTH, *A Review of a Posteriori Error Estimation and Adaptive Mesh Refinement Techniques*, Wiley, Chichester, 1996.